Journal of Porphyrins and Phthalocyanines
J. Porphyrins Phthalocyanines 2020; **24**: 456–464
DOI: 10.1142/S1088424619501785

Published at https://www.worldscinet.com/jpp/

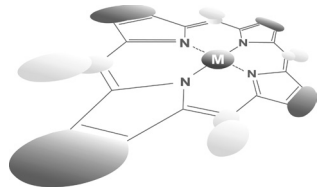

Synthesis of highly water soluble tetrabenzoporphyrins and their application toward photodynamic therapy

Austen Moss[†a], Zehua Zhou[†b], Lin Jiang*[c], M. Graça H. Vicente*[b◊] and Hong Wang*[a]

[a]*Department of Chemistry, University of North Texas, Denton, TX 76201, USA*
[b]*Department of Chemistry, Louisiana State University, Baton Rouge, LA 70803, USA*
[c]*Division of Natural Sciences, New College of Florida, Sarasota, FL 34243, USA*

Dedicated to Professor Atsuhiro Osuka on the occasion of his 65th birthday.

Received 6 July 2019
Accepted 13 November 2019

ABSTRACT: Novel tetraaryl-(pyridinium-4-yl)-tetrabenzoporphyrins have been successfully synthesized *via* a Heck-based sequence reaction. These tetrabenzoporphyrins were substituted with eight pyridyl groups at the fused benzene rings. Methylation of the pyridyl groups with methyl iodide afforded highly water soluble tetrabenzoporphyrins carrying eight ionic groups. The extended π-conjugation broadened and red-shifted the absorption band of these porphyrins to 650–750 nm. These cationic tetrabenzoporphyrins showed non-toxicity in the dark up to 100 uM. High phototoxicity with IC_{50} values lower than 18 μM were obtained for these tetrabenzoporphyrins.

KEYWORDS: tetrabenzoporphyrin, water solubility, DFT calculation, photosensitizer, PDT.

INTRODUCTION

Photodynamic therapy (PDT) has been established as an important tool for cancer treatment due to its less harmful side effects to normal cells compared to chemotherapy and radiotherapy. There are three major components in PDT: a photosensitizer, an appropriate source of visible or near-IR light, and oxygen in tissue. Upon irradiation, the excited state of the photosensitizer generates highly reactive singlet oxygen and other cytotoxic reactive oxygen species which can induce localized cell death and ultimately tissue apoptosis and/or necrosis [1–3]. PDT has been successfully applied to various cancers including brain tumors [4], esophageal cancers [5], early oral and laryngeal cancers [6], as well as breast carcinoma [7]. The most effective photosensitizers are those having strong absorption bands in the red region of the visible spectrum because both absorption and scattering of light by tissue decrease as the wavelength increases. On the other hand, the absorption bands should not be too far in the red region to avoid the decrease of the oxidation potential and photobleaching [8, 9]. Based on these two factors, the ideal photosensitizer should be activated at wavelengths between 700 to 850 nm for maximum light penetration through tissues with minimum light scattering [10].

Porphyrin-based photosensitizers have risen to prominence due to their selectivity or persistence in tumor cells [11–15]. However, porphyrin photosensitizers also have several disadvantages including poor light absorption in the ideal region, low solubility in aqueous media and cutaneous phototoxicity side effects. To solve these problems, new generations of porphyrins and porphyrin derivatives have been developed. These porphyrins such as Tookad [16], Photofrin [17], Lutrin [18], and Purlytin [19] (Fig. 1) absorb light at longer wavelengths with improved activity and minimized side effects [20, 21]. While

◊ SPP full member in good standing

*Correspondence to: Hong Wang, tel.: +940-369-8238, email: hong.wang@unt.edu; M. Graca H. Vicente, tel.: +225-578-7405, email: vicente@lsu.edu; Lin Jiang, tel.: +941-487-4315, email: ljiang@ncf.edu.
†These two authors contributed equally to the preparation of this manuscript.

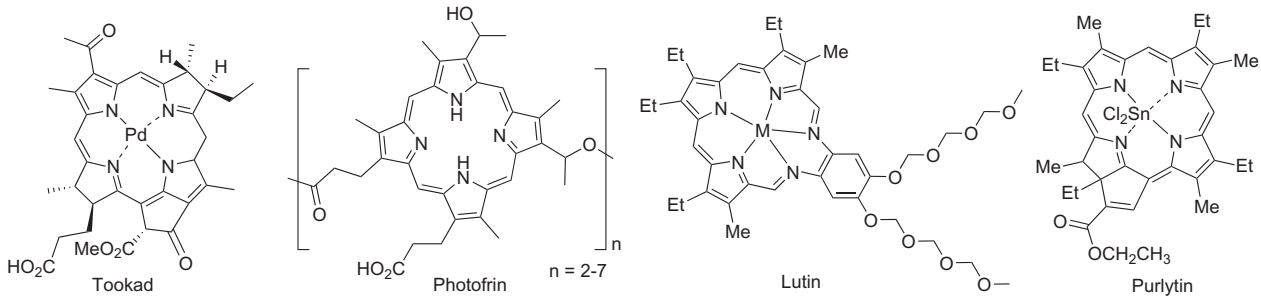

Fig.1. Structures of the porphyrin based photosensitizers used for clinical or preclinical photodynamic therapy

these impressive advances suggest the great potential of porphyrins in PDT, major drawbacks of porphyrin-based photosensitizers still exist. The search for new classes of porphyrin sensitizers still remain an intense research interest [22–27].

Tetrabenzoporphyins (TBPs), which have fused aromatic rings at the porphyrin β–pyrrolic positions, are attractive synthetic targets for PDT. TBPs generally display much broadened and red-shifted absorption bands relative to those of their corresponding unfused counterparts due to the π-extension. The range of Q band absorption of TBPs generally lies at 600–750 nm and are often enhanced, a much-desired feature for PDT applications. However, due to the poor solubility and limited synthetic methods, especially the lack of functionalization methods, only a small number of TBPs and their derivatives have been made available. Sugimoto and co-workers synthesized a TBP bearing eight carboxylic acid groups [28]. Although the carboxylic acid groups were expected to increase the water solubility of this porphyrin, severe aggregation caused by the highly planar structure due to lack of *meso*-substitution limited the application of this novel TBP in PDT. Introduction of aryl groups to the *meso*-positions of TBPs will result in much less planar structures and thus decrease the aggregation problems [29]. Recently, we have developed a concise and versatile method to synthesize β-functionalized *meso*-tetraarylbenzoporphyrins [30]. In this method, an alkene reacts with a β,β′-dibromoporphyrin through a three-step one pot sequence reaction involving a vicinal two-fold Heck reaction, six-π electrocyclization, and subsequent aromatization. In this work, we describe the synthesis, characterization and phototoxicity investigations of two highly water-soluble *meso*-tetraaryltetrabenzoporphyrins, $Ar_4[T(MPy)_8BP]I_8$. These tetrabenzoporphyrins were prepared through the Heck-based sequence reaction using 2-vinyl pyridine and β-octabromoporphyrin. Eight pyridyl groups were attached at the fused benzene rings of these TBPs [31]. Methylation of the pyridyl groups generated eight pyridinium iodide units, which make the TBPs highly water soluble.

EXPERIMENTAL

General methods

All solvents were analytical reagent grade and were obtained either from Sigma–Aldrich or ACROS. Analytical thin layer chromatography (TLC) was performed on Silicycle UltraPure Silica Gel 60 F254 TLC plates. ^{1}H and ^{13}C NMR experiments were conducted on a Bruker Avance 500 MHz spectrometer. Both samples were prepared in methanol-d_4 and chemical shifts were referenced to *d*-methanol at 3.31 ppm for ^{1}H NMR. UV-vis spectra were recorded on an Agilent 8453 UV-vis spectrometer in CH_2Cl_2. Fluorescence spectra were recorded on a PerkinElmer LS 55 fluorescence spectrometer. Mass spectra were obtained on a Bruker MALDI-TOF mass spectrometer.

Synthesis

Porphyrins **1**, **2** and **4** were prepared using procedures published previously [31].

[5,10,15,20-*tetrakis*[4-(*isopropyl*)*phenyl*]-*octakis*[*N-methylpyridinium*-4-*yl*]-*benzoporphyrinato*]*zinc*(II) *octaiodide* 3. To a solution of porphyrin **2** (25 mg, 15 μmol) in methanol (3 mL) was added an excess of iodomethane (1 mL, 16 mmol). The mixture was stirred vigorously at room temperature for two days. The solvent was evaporated under vacuum. Recrystallization from methanol and chloroform gave brownish crystals of the title porphyrin (40 mg, 95%). UV-vis λ_{max} (methanol)/nm 530 (log ε 5.30), 653 (3.98), 698 (4.23); ^{1}H NMR (500 MHz, CD_3OD, Me_4Si) δ 8.82–8.83 (16H, m), 7.87–8.31 (16H, m), 7.73–7.74 (16H, m), 7.32–7.46 (8H, m), 4.35–4.39 (24H, s, -CH_3), 3.39 (4H, m, isopropyl(CH)-H), 1.42 (24H, d, J = 6.5 Hz, isopropyl (CH_3)-H). MALDI-TOF-HRMS: calcd for $C_{120}H_{108}N_{12}Zn^{8+}$ 1780.81, found 1780.7806.

[5,10,15,20-*tetrakis*[4-(*isopropyl*)*phenyl*]-*octakis*[*N-methylpyridinium*-4-*yl*]-*benzoporphyrinato*]*octaiodide* 5. To a solution of porphyrin **4** (25 mg, 16 μmol) in methanol (3 mL) was added an excess of iodomethane (1 mL, 16 mmol). The mixture was stirred vigorously at room temperature for two days. The solvent was

evaporated under vacuum. Recrystallization from methanol and chloroform gave brownish crystals of the title porphyrin (41 mg, 96%). UV-vis λ_{max} (methanol)/nm 524 (log ε 5.29), 694 (4.20); ^{1}H NMR (500 MHz, CD_3OD, Me_4Si) δ 8.82–8.85 (16H, m), 8.52–8.76 (8H, m), 7.89–7.93 (8H, m), 7.75–7.76 (18H, m), 7.50–7.58 (6H, m), 4.40–4.42 (24H, s, -CH_3), 3.34 (4H, m, isopropyl(CH)-H), 1.46 (24H, d, J = 6.5 Hz, isopropyl (CH_3)-H). MALDI-TOF-HRMS: calcd for $C_{120}H_{110}N_{12}^{8+}$ 1718.89, found 1718.7313.

The study of biological properties

The HEp2 cell line used in this study was purchased from ATCC. The culture medium and reagents were purchased from Life Technologies. The HEp2 cells were cultured in the medium (DMEM: Advanced = 1:1) containing 10% FBS and 1% antibiotic (Penicillin-streptomycin). The Zn(II) and metal-free tetrabenzoporphyrins were synthesized as shown in Scheme 1 by Ms. James Winter. A 32 mM compound stock solution of each compound was prepared by dissolving the compound in DMSO (Sigma–Aldrich). The working solutions were prepared by diluting the 32 mM stock solution with the culture medium. All reagents and culture media were purchased from Thermofisher.

Time-dependent cellular uptake

The HEp2 cells were plated at 15000 cells per well in a Costar 96-well plate (BD biosciences) and grown overnight. The 10 μM compound working concentration was made by diluting 32 μM stock solution with a medium containing 5% FBS and 1% antibiotic. The cells were treated by adding 100 μL/well of 10 μM working solution at different time periods of 0, 1, 2, 4, 8, and 24 h. The loading medium was removed at the end of the treatments. The cells were washed with 1X PBS, and solubilized by adding 0.25% Triton X-100 in 1X PBS. A compound standard curve, 10 μM, 5 μM, 2.5 μM, 1.25 μM, 0.625 μM, 0.3125 μM, was made by diluting 32 μM compound solution with 0.25% Triton X-100 (Sigma–Aldrich) in 1X PBS. A cell standard curve was prepared using 10000, 20000, 40000, 60000, 80000, and 100000 cells per well. The cells were quantified by CyQuant Cell Proliferation Assay (Life Technologies). The compound and cell numbers were determined using a FluoStar Optima micro-plate reader (BMG LRBTEH), with wavelengths 520/720 nm for compound and 480/520 nm for cells, respectively. Cellular uptake is expressed in terms of nM compound per cell.

Cytotoxicity

Dark Toxicity: HEp2 cells were placed in a 96-well plate as above, with the compound concentrations of 100, 50, 25, 12.5, 6.25, and 0 μM, five repetitions for each concentration, and then incubated at 37 °C. After 24 h incubation, the compound was removed by washing cells with 1X PBS three times and replaced with media containing 20% Cell Titer Blue. The cells were

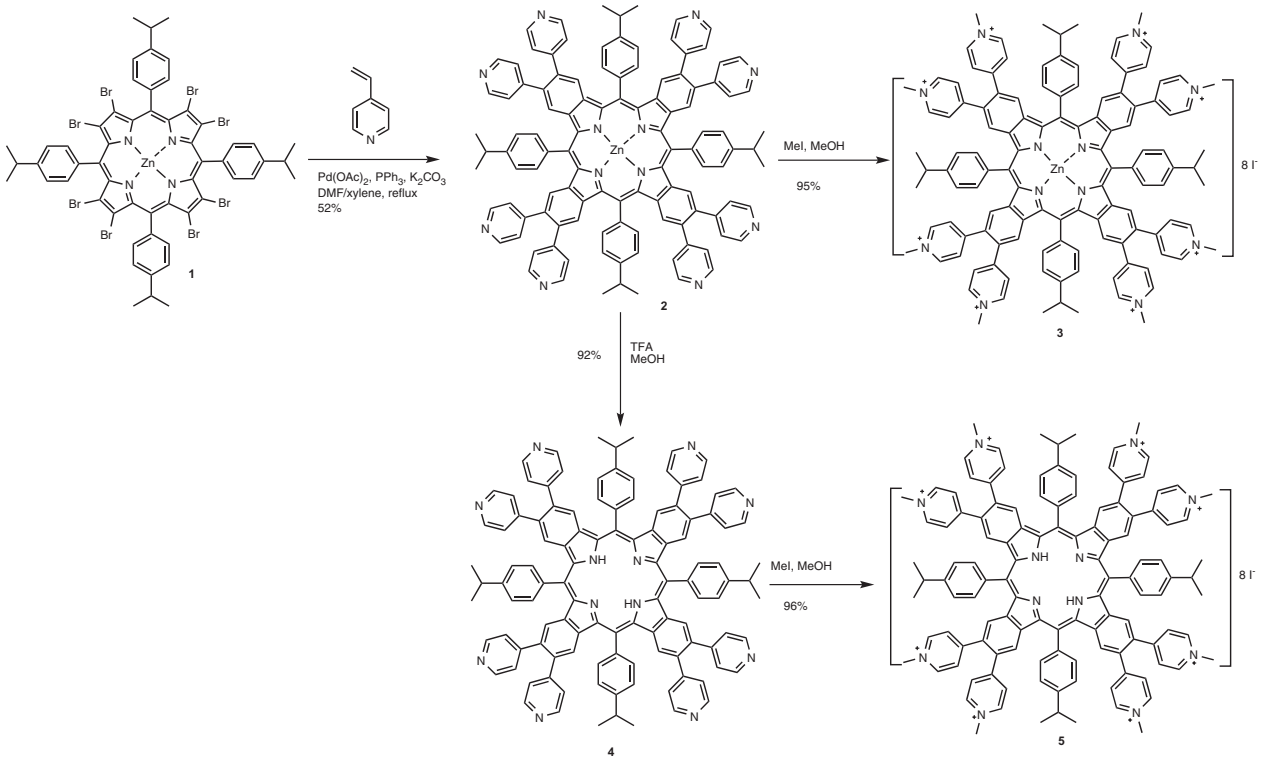

Scheme 1. Synthesis of water soluble tetrabenzoporphyrins

incubated for an additional 4 h at 37 °C. The viable cells were measured at 570/615 nm using a FluoStar Optima micro-plate reader. The dark toxicity is expressed in terms of the percentage of viable cells.

Phototoxicity. The concentrations of 100, 50, 25, 12.5, 6.25, 3.125, 1.5625, and 0 μM were used for the phototoxicity experiments. The HEp2 cells were placed in 96-well plates as described above and treated with compound for 24 h at 37 °C. After the 24 h treatment, the loading media was removed. The cells were washed with 1X PBS, and then refilled with fresh media. The cells were exposed to approximately 1.5 J/cm^2 light dose. After exposure to light, the cells were again incubated for 24 h. After the 24 h incubation, the medium was removed and replaced with media containing 20% Cell Titer Blue. The cells were incubated for an additional 4 h. The viable cells were measured as described above. The phototoxicity is expressed in terms of the percentage of viable cells.

Intracellular localization. The HEp2 cells were placed in 6-well plates, allowed to grow for 24–48 h, and then exposed to 10 μM concentration of the compound and incubated overnight. Molecular probes (tracers) were added and allowed to react for 30 min in a 37 °C incubator. The cells were washed with 1X PBS three times, and then refilled with 1X PBS 5 mL/well. The compound distribution was determined by using a Leica DM6B, an upright fluorescence microscope fitted with standard Texas Red, GFP, DAPI, filter sets. A water immersed objective was used to determine the compound localizations.

RESULTS AND DISCUSSION

Molecular design and synthesis

One strategy to enhance water solubility of a porphyrin compound is to attach ionic components to the porphyrin periphery. Porphyrins bearing pyridium groups appear to be good candidates to serve this purpose. Porphyrins with four pyridinium groups attached at the *meso* positions have been used as water-soluble porphyrins in various applications [32–35]. It can be envisioned that the water solubility of the porphyrins would be enhanced if more pyridium groups could be attached to the porphyrin periphery. Recently, our group developed a concise synthetic method to access benzoporphyrins through a Heck reaction-based one-pot sequence reaction [36]. Using this method, we were able to prepare TBPs bearing eight pyridyl groups substituted at the fused benzene rings, which provide easy access to water-soluble porphyrins. The synthesis of water-soluble zinc and free-base *octa*-(*N*-methylpyridinium-4-yl)-tetraaryl-tetrabenzoporphyrins **3** and **5** are illustrated in Scheme 1. Octabromoporphyrin **1** reacted with 2-vinylpyridine in the presence of *in situ*-formed Pd(0) catalyst through the Heck-based sequence reaction to afford zinc *octa*-pyridyl-tetraaryl-tetrabenzoporphyrin **2** in 52% yield [31]. Removal of zinc from **2** was performed with trifluoroacetic acid (TFA) in methanol, producing metal-free *octa*-pyridyl-tetraaryl-tetrabenzoporphyrin **4**. Tetrabenzoporphyrins **2** and **4** were then treated with MeI

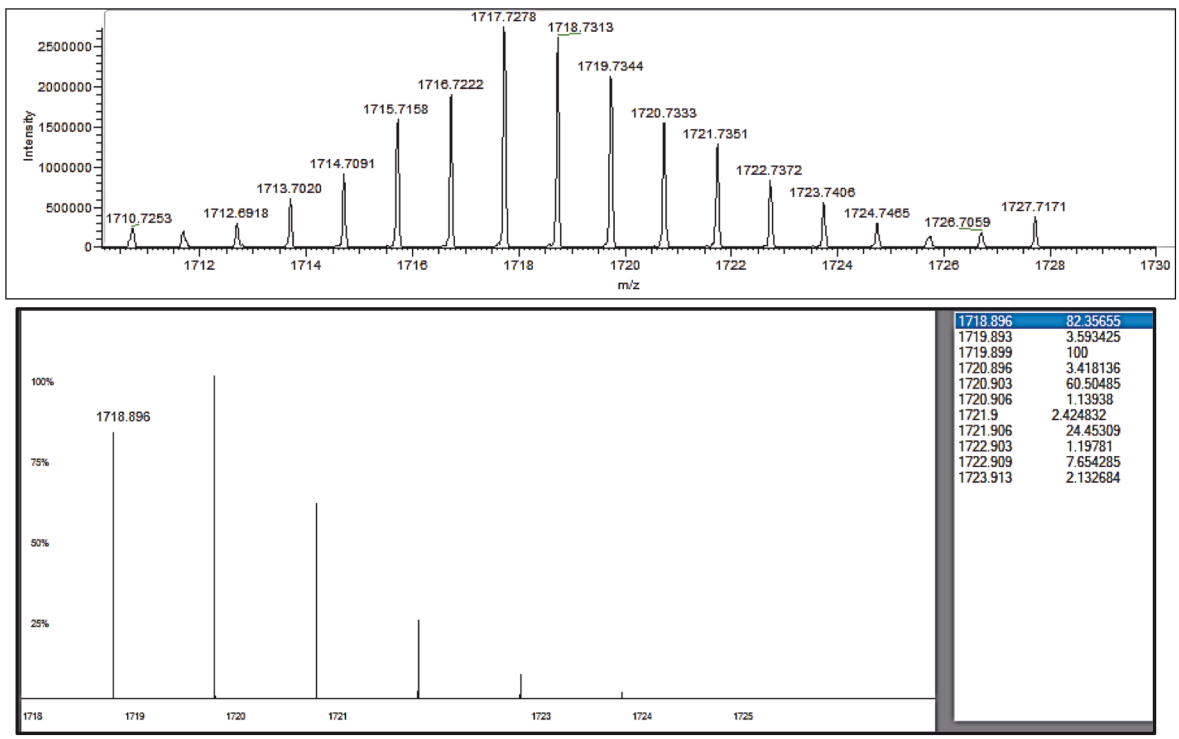

Fig. 2. MALDI-TOF mass spectrum of **5**

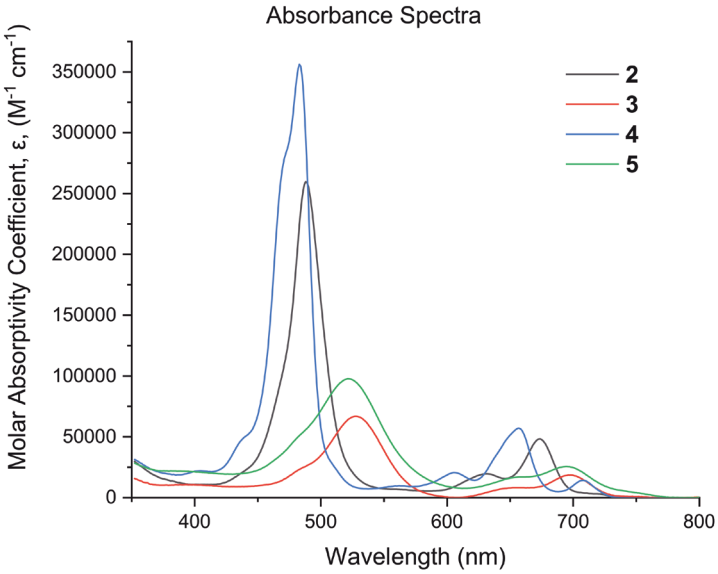

(a)

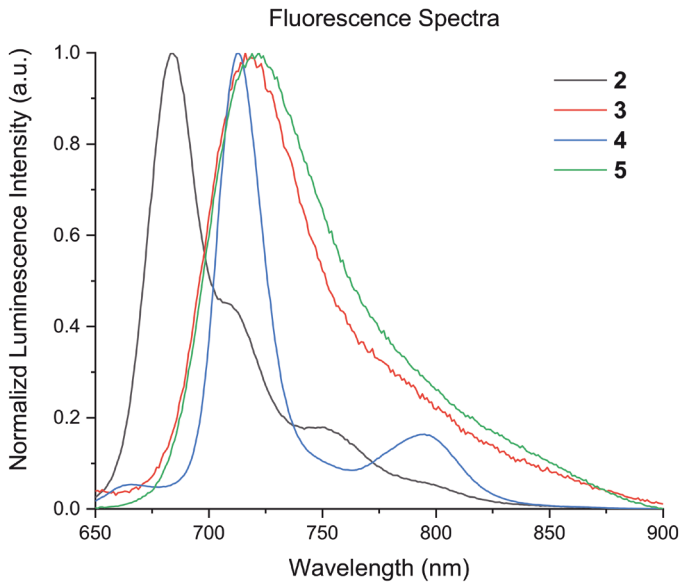

(b)

Fig. 3. (a) Normalized absorption spectra of porphyrins **2**–**5** (**2** and **4** were tested in CH_2Cl_2 solution; **3** and **5** were tested in methanol solution); (b) Fluorescent spectra of **3** and **5** in methanol

in methanol for two days at room temperature. The color of the solution changed from dark green to rosy/brownish. Upon removal of solvents, the resulting residues were recrystallized with chloroform/methanol. Tetrabenzoporphyrins **3** and **5** bearing eight pyridium groups were obtained in 95% and 96% yield, respectively. Tetrabenzoporphyrins **3** and **5** were highly soluble in water. Their aqueous solutions were stable for more than one week at room temperature when shielded from light. Precipitation was not observed visually. A stability study performed with UV-vis spectroscopy was consistent with the observation.

Mass spectrometry

Mass spectrometry of tetrabenzoporphyrins **3** and **5** was conducted using high resolution matrix assisted laser desorption ionization time-of-flight (MALDI-TOF) technique. Both compounds showed the expected peaks for **3** and **5** (see Fig. 2 and Fig. S9 in the Supporting information), confirming the successful preparation of **3** and **5**.

^{1}H NMR characterization

The ^{1}H NMR spectra of these compounds are included in the Supporting information (Figs S4–S8). It was expected that these porphyrins show 5 sets of aromatic proton shifts in the region of 6.5–9.0 ppm; compounds **2** and **4** should show 2 sets and compounds **3** and **5** should show 3 sets of proton shifts in the aliphatic region. Due to multiple dynamics occurring in these peripherally crowded porphyrin systems including ring flipping and ring rotations as well as solvation of the strongly polar groups and ionic groups in the porphyrins, it is tricky to obtain well-defined ^{1}H NMR spectra for these compounds. ^{1}H NMR of these compounds (**2**–**5**) in different solvents, *i.e.* methanol-d_4, $CDCl_3$ and DMSO-d_6, were acquired. Clean and well-defined ^{1}H NMR spectra for **2** and **3** were obtained, and the peaks were well-assigned. While the ^{1}H NMR spectra of **4** displayed the expected two sets of proton shifts in the aliphatic region, however, only 4 sets of protons in the aromatic region were identified. One set of proton shifts for the eight protons on the fused benzene ring is missing. Since **4** was obtained from **2** simply through demetallation, it is unlikely that the fused benzene rings were cut off during the reaction, while keeping all other components intact. We speculate that those very small peaks in the 7.00–7.75 ppm region account for the missed 8 H (on fused benzene rings) due to the ring dynamics. The speculation can be further confirmed with the ^{1}H NMR of **3**. Compound **3** was also obtained from **2** through methylation. Fortunately, the ^{1}H NMR spectra acquired for **3** show well-defined and well-assigned proton shifts in the aromatic region. All these data together confirm the identity and purity of compounds **2**, **3** and **4**. Compound **5** was prepared from **4**. ^{1}H NMR spectra for **5** were acquired in both methanol-d_4 and DMSO-d_6. Not surprisingly, the two ^{1}H NMR spectra appeared to be very different (Figs S4 and S5), proving our above mentioned hypothesis of ongoing multiple dynamics in the system affecting the proton shifts on ^{1}H NMR spectra. Although on both spectra the peaks in the aromatic region are not well-defined, proton shifts in the

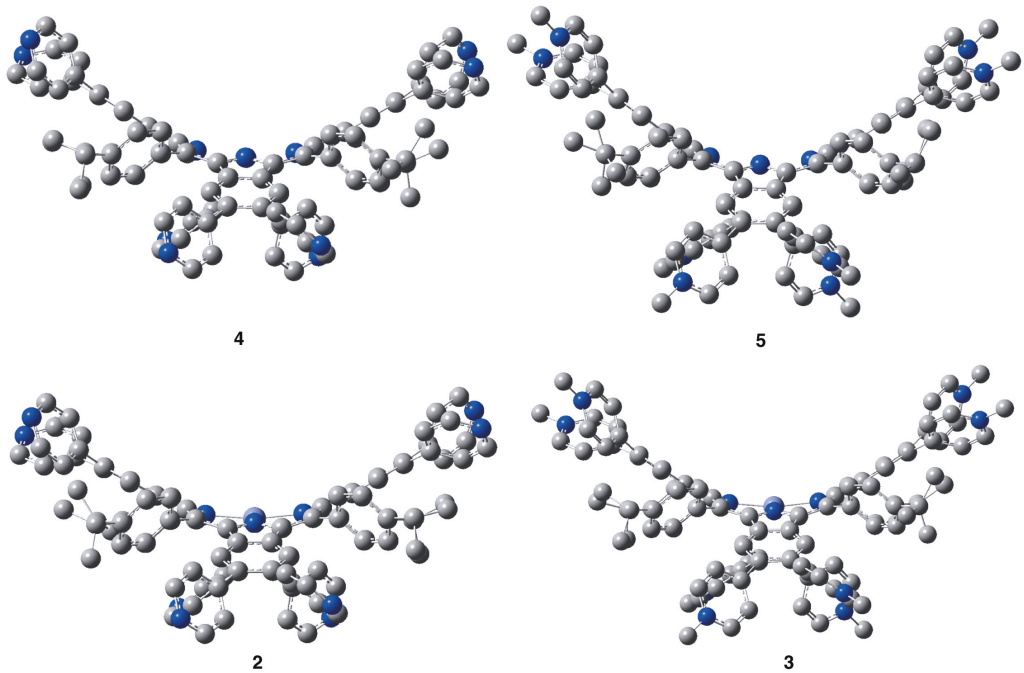

Fig.4. Optimized geometries of porphyrin **2–5**

aliphatic region are well-defined and can be undoubtedly assigned. Based on the analysis, we are confident with the identity and purity of compound **5**.

Optical properties

UV-vis absorption spectra of **2–5** are compiled in Fig. 3(a). The Soret bands of tetrabenzoporphyrins **2** and **4** were found at 484 nm and 492 nm, respectively, which are significantly broadened and red-shifted relative to those of simple corresponding tetraarylporphyrins (~419–424 nm) due to the fusion of the benzene rings to the porphyrin periphery. Upon methylation of the pyridyl rings, the Soret bands are further broadened and red-shifted by another 30 to 40 nm to 530 nm (**3**) and 524 nm (**5**). The Q bands of **2–5** are also broadened and red-shifted to red/near IR region. The Q bands of all these tetrabenzoporphyrins are much enhanced. The enhancement of the Q bands is even more pronounced for the ionic porphyrins **3** and **5**. The fluorescence spectra of **3** and **5** displayed near IR emissions (Fig. 3(b)). Singlet oxygen production of **3** and **5** was measured using luminescence spectroscopy (see Figs S1–S3). Both compounds displayed singlet oxygen production.

DFT calculation

The molecular geometries of these porphyrins was optimized using density functional theory calculations (B3LYP, 6-31G(d,p)). As illustrated in Fig. 4, all these porphyrins show a saddle-like conformation. These molecules are significantly deviated from planarity due to the steric crowding of the eight pyridyl rings on the porphyrin periphery. As a result, the aggregation problems often observed for tetrabenzoporphyrins are significantly alleviated in this case. The free base and zinc octapyridyl-tetrabenzoporphyrins dissolve well in a large range of organic solvents including polar and non-polar solvents such as chloroform, toluene and methanol. The methylated free base and zinc octapyridyl-tetrabenzoporphyrins are readily soluble in water and methanol.

Cellular studies

Cytotoxicity and the uptake of tetrabenzoporphyrins **3** and **5** in human HEp2 cells were investigated, and the results obtained are shown in Figs. 5–9 and Tables 1 and 2.

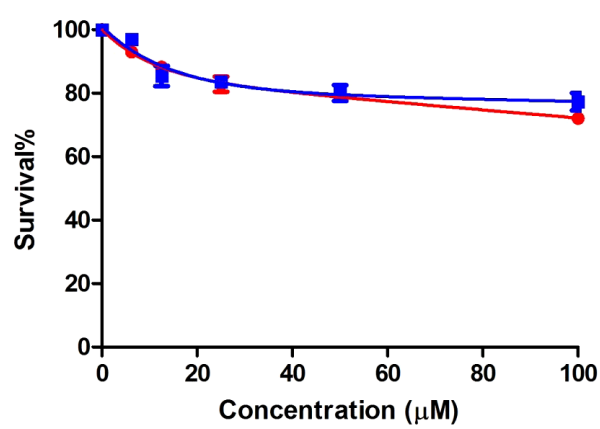

Fig. 5. Dark cytotoxicity of tetrabenzoporphyrins **3** (red) and **5** (blue) in human HEp2 cells

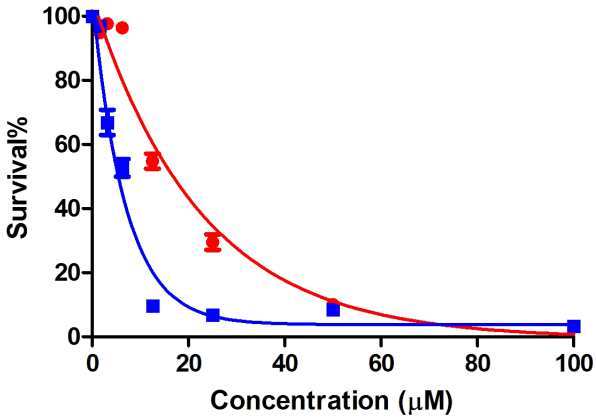

Fig.6. Phototoxicity (~1.5 J/cm^2) of tetrabenzoporphyrins **3** (red) and **5** (blue) in human HEp2 cells

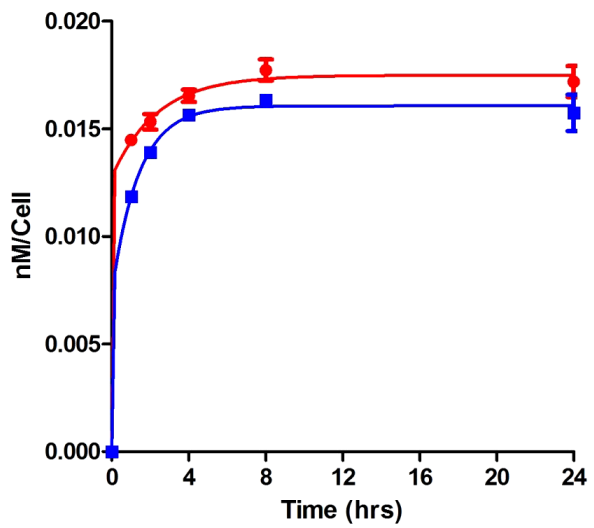

Fig. 7. Time-dependent uptake of tetrabenzoporphyrins **3** (red) and **5** (blue) at 10 uM by human HEp2 cells

The cytotoxicity was evaluated using a Cell Titer Blue assay, at concentrations up to 100 uM. Both cationic tetrabenzoporphyrins were found to be non-toxic in the dark up to 100 uM, but they were highly phototoxic at approximately 1.5 J/cm^2 light dose, with calculated IC_{50} values of 17 and 6.25 uM for **3** and **5**, respectively (see Fig. 6 and Table 1). Both tetrabenzoporphyrins were taken up by the HEp2 cells very rapidly in the first 2 h, after which a plateau was observed (see Fig. 7). The subcellular localization of the compounds was investigated by fluorescence microscopy upon exposure of HEp2 cells to 10 μM compound concentrations for about 6 h. The organelle-specific fluorescence probes BODIPY Ceramide (Golgi), Lyso-Sensor Green (lysosomes), Mito-Tracker Green (Mitochondria), and ER Tracker Blue/White (ER) (Invitrogen) were used in the experiments. Both compounds localized mainly in the ER and Golgi apparatus, and were also observed,

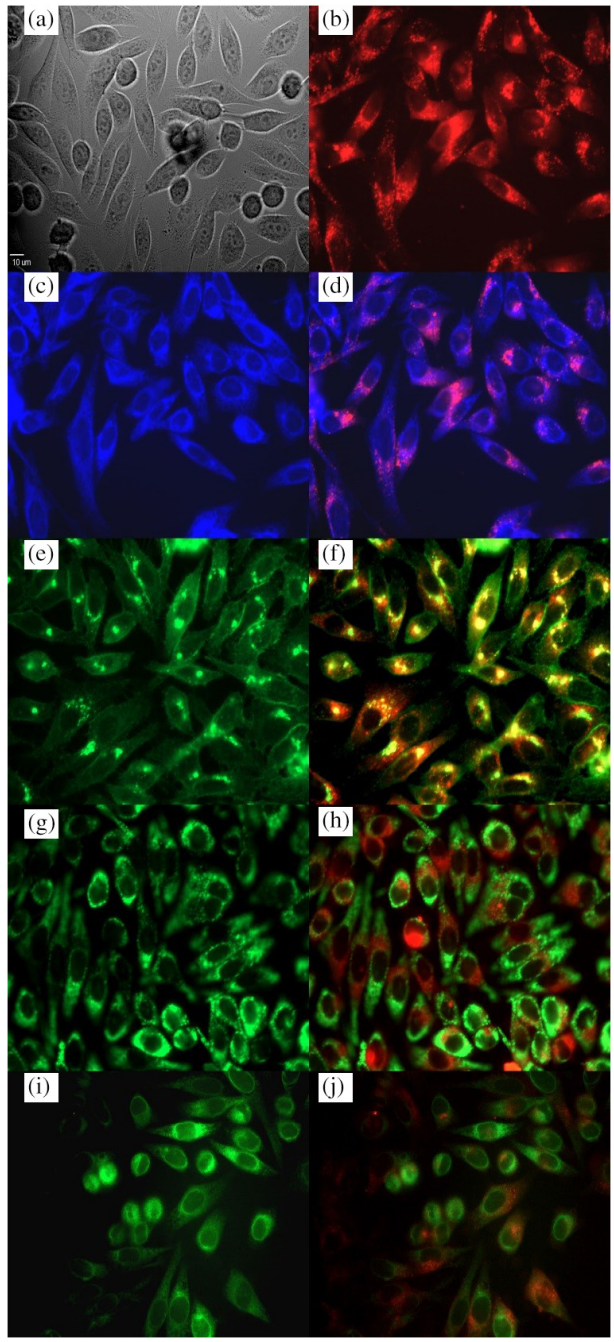

Fig. 8. Subcellular distribution of **3** in HEp2 cells at 10 μM for 6 h. (a) Phase contrast, (b) the fluorescence of compound **3**, (c) ER Tracker Blue/White, (d) overlay of **3** and ER Tracker, (e) BODIPY Ceramide, (f) overlay of **3** and BODIPY Ceramide, (g) MitoTracker Green, (h) overlay of **3** and MitoTracker, (i) LysoSensor Green, and (j) overlay of **3** and LysoSensor Green. Scale bar: 10 μm

although in a smaller extent, in the lysosomes and mitochondria (see Figs 8 and 9 and Table 2).

These studies show that the metal-free tetrabenzoporphyrin **5** is more phototoxic than the corresponding Zn(II) complex **3**, although the Zn(II) complex **3** was

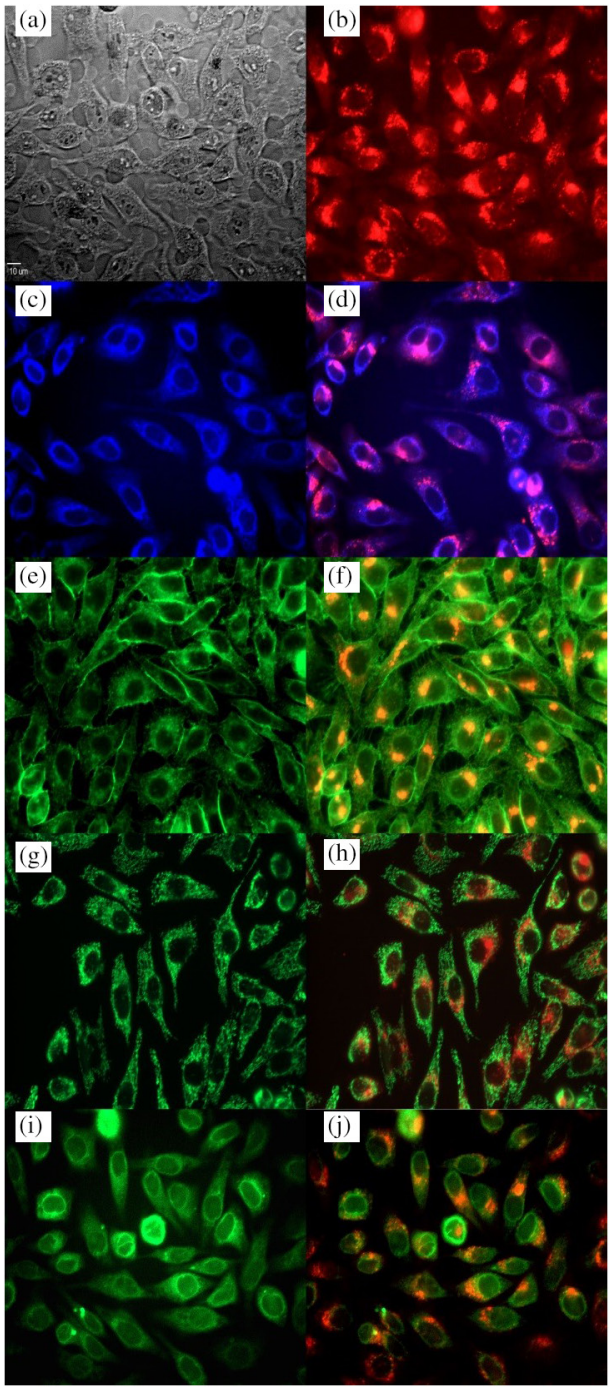

Fig. 9. Subcellular distribution of **5** in HEp2 cells at 10 μM for 6 h. (a) Phase contrast, (b) the fluorescence of compound **3**, (c) ER Tracker Blue/White, (d) overlay of **3** and ER Tracker, (e) BODIPY Ceramide, (f) overlay of **3** and BODIPY Ceramide, (g) MitoTracker Green, (h) overlay of **3** and MitoTracker, (i) LysoSensor Green, and (j) overlay of **3** and LysoSensor Green. Scale bar: 10 μm

taken up more efficiently by the cells. The observed difference in phototoxicity might be due to the subcellular distribution of these two compounds and their ability for generating singlet oxygen. The metal-free **5** was found

Table 1. Cytotoxicity (Cell Titer Blue assay, 1.5 J/cm^2)

Compound	Dark toxicity (IC_{50}, μM)	Phototoxicity (IC_{50}, μM)
3	>100	17
5	>100	6.25

Table 2. Major (+++) and minor (+) subcellular sites of localization in HEp2 cells

Compound	Er	Golgi	Mitochondria	Lysosomes
C1	++	+++	+	+
C2	+++	++	+	+

in a greater amount in the ER, while the Zn(II) complex **3** was mainly found in the Golgi apparatus (Table 2). The ER is an important PDT target, and enhanced accumulation in this organelle can lead to rapid cell death due to photodamage to anti-apoptotic Bcl-2 proteins. In addition, tetrabenzoporphyrin **3** is expected to have decreased hydrophobicity compared with the metal-free base tetrabenzoporphyrin **5**, which could also account for the observed difference in phototoxicity.

CONCLUSION

In this study, we described a concise synthetic method affording highly water soluble $Ar_4[T(MPy)_8BP]I_8$ type tetrabenzoporphyrins. With eight ionic groups on β-positions of the porphyrin periphery, these compounds are highly soluble in water and methanol. The UV-vis spectra of these porphyrins displayed significantly red-shifted and broadened Soret bands and Q bands, making the absorption spectra cover almost the whole visible region. Near-IR fluorescence from 700 to 870 nm provided ideal data for penetration depth. These interesting data have never been discovered in other types of water-soluble porphyrins. This method can be used to introduce a variety of counter ions on the eight pyridine rings. Compared with known TBPs in PDT [28, 29], this novel class of $Ar_4[T(MPy)_8BP]I_8$ porphyrins displayed more promising UV-vis and fluorescence data. These water-soluble tetrabenzoporphyrins showed uptake into human carcinoma HEp2 cells, and were found localized mainly in the ER and Golgi apparatus. The presence of these compounds was also observed in the lysosomes and mitochondria. Both cationic tetrabenzoporphyrins displayed non-toxicity in the dark up to 100 uM, and high phototoxicity at approximately 1.5 J/cm^2 light dose, with calculated IC_{50} values of 17 and 6.25 uM for **3** and **5**, respectively.

Acknowledgments

The U.S. Department of Energy, Office of Science, Basic Energy Sciences (DE-SC0016766) supported

research conducted by LJ, AM and HW at University of North Texas. The National Science Foundation (CHE-1800126) supported the work conducted by ZZ, MGHV. We thank Dr. Guido Verbeck and the Laboratory for Imaging Mass Spectrometry at the University of North Texas for MALDI-Orbitrap Mass Spectrometry data.

Supporting information

^{1}H NMR and MS spectroscopic data are given in the supplementary material. This material is available free of charge *via* the Internet at http://www.worldscinet.com/jpp/jpp.shtml.

REFERENCES

1. Kessel D. *Photodiagn. Photodyn. Ther.* 2004; **1**: 3–7.
2. Dougherty T, Gomer C, Henderson B, Jori G, Kessel D, Korbelik M, Moan J and Peng Q. *J. Natl. Cancer Inst.* 1998; **90**: 889–905.
3. Moan J and Peng Q. *Anticancer Res.* 2003; **23**: 3591–3600.
4. Powers S, Cush S, Walstad D and Kwock L. *Neurosurgery* 1991; **29**: 688–696.
5. Marcon N. *Semin. Oncol.* 1994; **21**: 20–23.
6. Biel M. *Photochem. Photobiol.* 2007; **83**: 1063–1068.
7. Allison R, Mang T, Hewson G Snider W and Dougherty D. *Cancer* 2001; **91**: 1–8.
8. Bonnett R. *Chemi. Soc. Rev.* 1995; **24**: 19–33.
9. Balaz M, Collins H, Dahlstedt E and Anderson H. *Org. Biomol. Chem.* 2009; **7**: 874–888.
10. O'Connor A, Gallagher W and Byrne A. *Photochem. Photobiol.* 2009; **85**: 1053–1074.
11. Gottumukkala V, Ongayi O, Baker D, Lomax L and Vicente M. *Bioorg. Med. Chem.* 2006; **14**: 1871–1879.
12. Thomas AP, Saneesh Babu PS, Asha Nair S, Ramakrishnan A, Ramaiah D, Chandrashekar TK, Srinivasan A and Radhakrishna Pillai M. *J. Med. Chem.* 2012; **55**: 5110–5120.
13. Schmitt F, Barry NPE, Juillerat-Jeanneret L and Therrien B. *Bioorg. Med. Chem. Lett.*2012; **22**: 178–180.
14. Orlandi VT, Caruso E, Banfi S and Barbieri P. *Photochem. Photobiol.* 2012; **88**: 557–564.
15. Dosselli R, Tampieri C, Ruiz-González R, De Munari S, Ragàs X, Sánchez-García D, Agut M, Nonell S, Reddi E and Gobbo M. *J. Med. Chem.* 2012; **56**: 1052–1063.
16. Weersink R, Bogaards A, Gertner M, Davidson S, Zhang K, Netchev G, Trachtenberg J and Wilson B. *J. Photochem. Photobiol., B* 2005; **79**: 211–222.
17. Karotki A, Khurana M, Lepock J and Wilson B. *Photochem. Photobiol.* 2006; **82**: 443–452.
18. Hsi R, Kapatkin A, Strandberg J, Zhu T, Vulcan T, Solonenko M, Rodriguez C, Chang J, Saunders M, Mason N and Hahn S. *Clin. Cancer Res.* 2001; **7**: 651–660.
19. Josefsen LB and Ross WB. *Met. -Based Drugs* 2008; **2008**: 1–24.
20. Koudinova N, Pinthus J, Brandis A, Brenner O, Bendel P, Ramon J, Eshhar Z, Scherz A and Salomon Y. *Int. J. Cancer* 2003; **104**: 782–789.
21. Liang X, Li X, Yue X and Dai Z. *Angew. Chem., Int. Ed.* 2011; **50**: 11622–11627.
22. Bhupathiraju N, Rizvi W, Batteas JD and Drain CM. *Org. Biomol. Chem.* 2016; **14**: 389–408.
23. Glowacka-Sobotta A, Wrotynski M, Kryjewski M, Sobotta L and Mielcarek J. *J. Porphyrins Phthalocyanines* 2019; **23**: 1–10.
24. Luciano M and Bruckner C. *Molecules* 2017; **22**: 980.
25. Rury AS, Wiley TE and Sension RJ. *Acc. Chem. Res.* 2015; **48**: 860–867.
26. Sandland J and Boyle RW. *Bioconjugate Chem.* 2019; **30**: 975–993.
27. Singh S, Aggarwal A, Bhupathiraju NV, Arianna G, Tiwari K and Drain CM. *Chem. Rev.* 2015; **115**: 10261–10306.
28. Murashima T, Tsujimoto S, Yamada T, Miyazawa T, Uno H, Ono N and Sugimoto N. *Tetrahedron Lett.* 2005; **46**: 113–116.
29. Menard F, Sol V, Ringot C, Granet R, Alves S, Le Morvan C, Queneau Y, Ono N and Krausz P. *Bioorg. Med. Chem.* 2009; **17**: 7647–7657.
30. Deshpande R, Jiang L, Schmidt G, Rakovan J, Wang X, Wheeler K and Wang H. *Org. Lett.* 2009; **11**: 4251–4253.
31. Jiang L, Zaenglein R, Engle J, Mittal C, Hartley CS, Ziegler C and Wang H. *Chem. Commun.* 2012; **48**: 6927–6929.
32. Ikeda A, Satake S, Mae T, Ueda M, Sugikawa K, Shigeto H, Funabashi H and Kuroda A. *ACS Med. Chem. Lett.* 2017; **8**: 555–559.
33. Sour A, Jenni S, Orti-Suarez A, Schmitt J, Heitz V, Bolze F, Loureiro de Sousa P, Po C, Bonnet CS, Pallier A, Toth E and Ventura B. *Inorg. Chem.* 2016; **55**: 4545–4554.
34. Zhang J-X, Li H, Chan C-F, Lan R, Chan W-L, Law G-L, Wong W-K and Wong K-L. *Chem. Commun.* 2012; 9646–9648.
35. Garcia-Sampedro A, Tabero A, Mahamed I and Acedo P. *J. Porphyrins Phthalocyanines* 2019; **23**: 16–27.
36. Deshpande R, Jiang L, Schmidt G, Deshpande R, Jiang L, Schmidt G, Rakovan J, Wang X, Wheeler K and Wang H. *Org. Lett.* 2009; **11**: 4251–4253.